Open access • Journal Article • DOI:10.1002/1616-3028(200106)11:3<179::AID-ADFM179>3.0.CO;2-5

The Growth of Transition Metals on H-Passivated Si(111) Substrates

— Source link

Jan O. Hauch, M. Fonine, U. May, R. Calarco ...+4 more authors

Institutions: RWTH Aachen University

Published on: 01 Jun 2001 - Advanced Functional Materials (WILEY-VCH Verlag GmbH)

Topics: Thin film, Giant magnetoresistance, Magnetoresistance and Ultra-high vacuum

Related papers:

- Scanning Tunneling Microscopy of the Initial Stages of Metal Condensation on Semiconductor Surfaces Progress Report
- The Role of Hydrogen in Metal/Si Interface Formation
- Impact of a-Si:H structural properties on the annealing behavior of a-Si:H/c-Si heterostructures used as precursors for high-efficiency solar cells
- Electron Spin Resonance Characterization of Defects at Interfaces in Stacks of Ultrathin High-κ Dielectric Layers on Silicon
- Improved interfacial local structural ordering of epitaxial Fe3Si(001) thin films on GaAs(001) by a MgO(001) tunneling barrier

Share this paper:

View more about this paper here: https://typeset.io/papers/the-growth-of-transition-metals-on-h-passivated-si-111-5ayb7z1px9

First publ. in: Advanced Functional Materials 11 (2001), 3, pp. 179-185

The Growth of Transition Metals on H-Passivated Si(111) Substrates**

By *Jan O. Hauch*, *Mikhail Fonine*, *Ulrich May*, *Raffaella Calarco*, *Harish Kittur*, *Jin M. Choi*, *Ulrich Rüdiger*,* and *Gernot Güntherodt*

The growth of Co and Ag layers on wet-processed H-passivated Si(111) substrates by molecular beam epitaxy (MBE) has been studied using high resolution scanning tunneling microscopy (STM) with regard to possible applications of the layers in magnetoelectronic devices. Roughness and intermixing at interfaces as functions of deposition temperature and layer thickness are key parameters for the performance of such devices. The initial growth of Co and Ag and the influence of Ag atoms on the Si(111) surface reconstructions provide insight into adatom–substrate interactions.

1. Introduction

To optimize the structure–property relationship of layered systems exhibiting giant magnetoresistance (GMR)[1–3] or tunneling magnetoresistance (TMR),[4–6] there is a call for textured or epitaxial ferromagnetic layers deposited on semiconductor substrates. For high-performance GMR and TMR devices the interface properties (roughness, electronic interface states, spin polarization, phase purity, etc.) of the ferromagnetic/non-ferromagnetic metal layers (GMR) and ferromagnetic metal/insulator hybrid structures (TMR) play a crucial role.

Currently, the "state-of-the-art" theoretical models for GMR[7–9] and TMR systems[10,11] are mainly developing calculations for epitaxial layers. Therefore the experimental investigation of epitaxial model systems becomes indispensable.

In order to grow high-quality (textured or epitaxial) Co thin films on oxide-free Si substrates the possible advantages of H-passivated Si(111) substrates have been explored. The latter can be prepared by "ex situ" wet-chemical processes and introduced easily into ultra high vacuum (UHV). The most reliable and reproducible results have been achieved on H-passivated Si(111) surfaces,[12] although this crystal orientation may not yield continuous epitaxial growth of face-centered cubic (fcc) metal layers.[13,14] In order to avoid silicide formation at the Co–Si interface, the influence of Ag buffer layers has been investigated.

The influence of Ag deposition at elevated temperatures ("hot" Ag deposition at T = 550 °C) on the formation of Si(111)-(2n+1)×(2n+1) reconstructions will be discussed and compared with the results of the reconstruction formation on a H-Si(111) surface after H-desorption by thermal annealing. The influence of Ag deposited at a lower temperature ("cold" Ag deposition at T = 250 °C) on the "wet prepared" H-Si(111) surface has also been investigated and compared with the hot Ag deposition at 550 °C on H-Si(111).

In this paper, growth modes of Co and Ag on H-passivated Si(111) substrates will be presented and discussed with regard to possible applications for magnetoelectronic devices.[15,16]

2. Results and Discussion

After introduction of a wet-chemically prepared monohydride Si(111)-(1×1) substrate into UHV, the quality and cleanliness of the surface were checked by scanning tunneling microscopy (STM) and Auger electron spectroscopy (AES). The Auger spectra of wet-chemically etched H-Si(111) substrates show a typical Si Auger LMM transition peak at an energy of 92 eV. The Auger intensities of carbonates and oxygen, which are the main contaminants, are negligible. From the Auger spectra one can conclude that the samples are clean on a macroscopic scale.

Figure 1 shows a STM image of a H-passivated Si(111) surface of 1000 nm × 1000 nm. The triangular shape of the H-Si(111) surface is due to the anisotropic etching rates along the

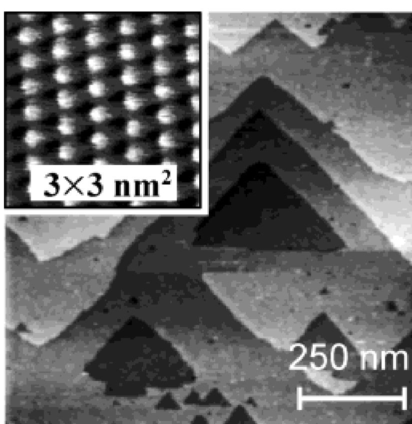

Fig. 1. STM image of large-area, triangular terraces of a wet-chemically processed H-terminated Si(111) surface. The inset shows that the monohydride termination leads to a H-Si(111)-(1×1) surface.

[*] Dr. U. Rüdiger, J. O. Hauch, M. Fonine, Dr. U. May, Dr. R. Calarco, H. Kittur, Dr. J. M. Choi, Prof. G. Güntherodt
II. Physikalisches Institut, RWTH Aachen
D-52056 Aachen (Germany)
E-mail: ruediger@physik.rwth-aachen.de

[**] This work was supported by Innovationsprogramm Forschung Forschungsverbund "Nanowissenschaften" of Nordrhein-Westfalen. J. M. Choi thanks the DAAD, Germany, and KOSEF, Korea, for financial support.

Konstanzer Online-Publikations-System (KOPS)
URL: http://www.ub.uni-konstanz.de/kops/volltexte/2008/5302/
URN: http://nbn-resolving.de/urn:nbn:de:bsz:352-opus-53029

[111]- and [100]-microfacet directions.[17] The step height was determined to be 3.1 Å, which corresponds to the height of one Si double layer, which is typical for the Si(111) surface. The atomically flat triangular terraces of the wet-chemically prepared H-Si(111)-(1×1) surface extend over hundreds of nanometers with no evidence of significant contamination. The inset in Figure 1 shows the atomically resolved H-passivated Si(111) surface with a lattice constant of 3.89 Å.

The outstanding surface properties and the "easy-to-handle" H-passivation procedure of Si(111) substrate surfaces make them promising templates for investigating growth and texture of ferromagnetic transition metals for application in magneto-electronic devices on the basis of established Si-technology.

2.1. Co-Growth at Room Temperature

Figure 2a shows a STM image of a H-Si(111) surface with nominally 0.5 monolayers (ML) of Co deposited at room temperature (RT). The STM image reveals an island-like growth on

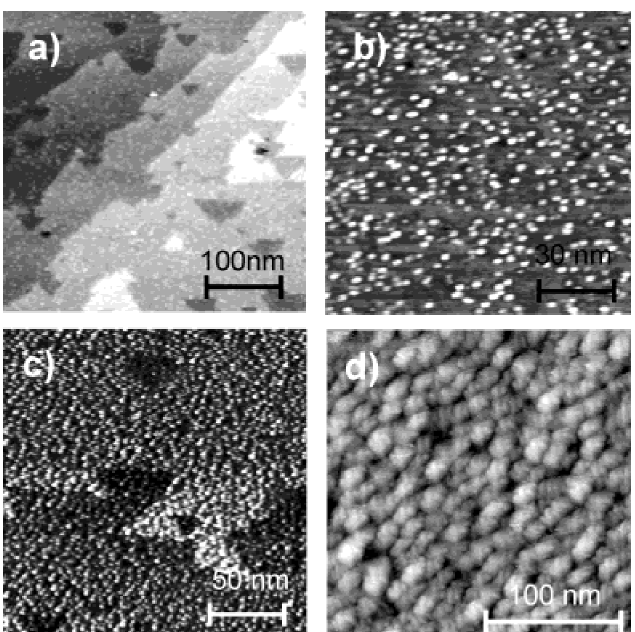

Fig. 2. H-passivated Si(111) surface covered at RT by nominally a) 0.5 ML Co, b) 1 ML Co, c) 7 ML Co, and d) 100 ML Co.

the triangular, atomically flat H-Si(111) substrate surface. The islands have an average diameter of 30–50 Å and an average height of 5.5 Å. The coverage of the surface was determined to be approximately 12 %. The STM image clearly identifies a Vollmer–Weber growth mode for the Co on the H-Si(111) surface at RT. As the nominal thickness is increased from 1 ML (Fig. 2b) to 7 ML (Fig. 2c), the growth and evolution of the Co cluster size and density as well as the roughness can be shown. Figure 2b shows a 120 nm × 120 nm region of the H-Si(111) surface covered by nominally 1 ML Co at RT. The diameter of the Co clusters is around 40 Å and the peak-to-peak roughness of 5.5 Å is in the same range as in Figure 2a. In Figure 2c (nominally 7 ML Co, grown at RT, scan size 200 nm × 200 nm) the clusters start to merge, causing an increase of the peak-to-peak roughness to 6.5 Å. The observed strong cluster formation of the deposited Co clusters is probably due to the weak Co–substrate interaction across the hydrogen atoms of the H-passivated Si(111) surface and the large lattice mismatch between the Co(0001) surface with a lattice constant of 2.54 Å and the Si(111) surface with 3.89 Å. The Co–Co binding energy of approximately 1 eV[18] is much larger than the van der Waals–like H–Co interaction. The large surface diffusion of Co atoms at RT supports the tendency of Co cluster formation.[19] H-desorption due to the presence of Co atoms on top of the H-passivation layer was not observed with STM imaging. In the case of H-desorption, Si dangling bonds would lead to a strong contrast in the STM images of the H-Si(111) surface.

Finally, Figure 2d shows a STM image of a 200 Å thick Co layer on H-Si(111) deposited at RT. The average lateral size of the Co clusters is about 300 Å × 180 Å. The peak-to-peak roughness was determined to be 18 Å. The STM image clearly exhibits an anisotropic in-plane growth of the Co clusters, but the growth anisotropy of the Co clusters has not yet been successfully correlated with the sixfold in-plane symmetry of the H-Si(111) substrate surface. The resulting roughness of a 200 Å thick Co layer is comparable with the typical thickness of the insulator barrier (10–20 Å) in magnetic tunnel junctions. This may cause problems in depositing pinhole-free, homogeneous insulator layers on top of the bottom electrode of such tunnel junctions using this type of H-passivated Si(111) substrates.

The Co growth at RT was also examined by reflection high energy electron diffraction (RHEED). In Figure 3a a RHEED

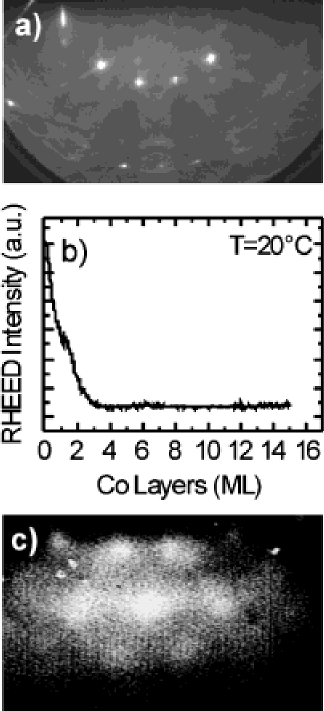

Fig. 3. a) The RHEED pattern with reflection spots on Laue circles demonstrates a flat and well-ordered H-Si(111) surface. b) The RHEED intensity of the 10 reflection as a function of Co coverage shows an exponential decrease, which is due to the 3D growth of Co islands. c) The sixfold symmetry of the 3D RHEED pattern of a nominally 15 ML thick Co layer indicates a slight *c*-axis orientation of the Co clusters.

pattern of a pure H-Si(111) substrate is shown. The position of reflection spots on Laue circles is an indication of a flat and well-ordered H-Si(111) surface, as was also seen in the STM investigation of the substrates. Figure 3b shows the RHEED intensity of the 10 spot during the growth of nominally 15 ML Co. A rapid drop of the RHEED intensity within the first 3 ML is due to three-dimensional (3D) island growth of Co on H-passivated Si(111) substrates, corresponding to the accumulated roughness with increasing Co thickness, as was also observed in the STM studies. After deposition of nominally 15 ML Co, a 3D RHEED pattern appears, indicating a weak texture of the Co clusters (see Fig. 3c). The large lattice mismatch between the Co(0001) surface with a lattice constant of 2.54 Å and the Si(111) surface with 3.89 Å makes a simple in-plane relationship of the two types of surface orientations unlikely.

2.2. Co-Growth at Elevated Temperature

In order to reduce the roughness of a thick Co film, Co was deposited at an increased substrate temperature. H-passivated Si substrates were used in an attempt to avoid the well-known cobalt silicide, $CoSi_x$, formation at higher temperatures.[20] Figure 4 shows a STM image of nominally 1 ML Co on H-passivated Si(111) deposited at a substrate temperature of 100 °C (scan size 156 nm × 156 nm). The cluster-like growth mode is

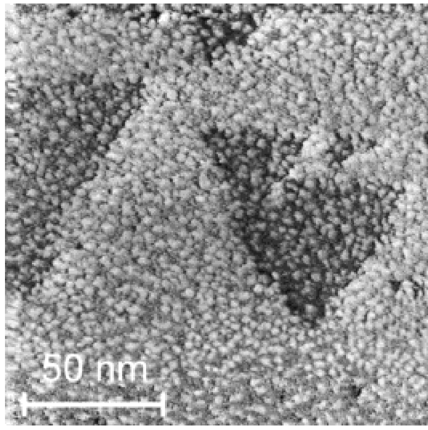

Fig. 4. STM image of nominally 1 ML Co on H-Si(111) deposited at T = 100 °C. Beside the Co cluster formation a significant change of the H-Si(111) surface topography appears due to $CoSi_x$ formation.

similar to the growth at RT. The clusters exhibit a height and diameter distribution comparable to that for the RT growth (see Fig. 2b). Beside the Co cluster formation, the topography (roughness) of the underlying H-passivated Si(111) substrate surface has changed dramatically. It was concluded that during the high temperature growth of Co the H–Si bonds break and $CoSi_x$ formation takes place. AES investigation of a 200 Å thick Co film also showed the presence of Si atoms within the probed depth, indicating $CoSi_x$ formation during the growth of the Co film at a temperature of 100 °C. The change of the magnetic bulk and surface properties of Co electrodes due to $CoSi_x$ formation is detrimental for the application of such a growth process in fabricating magnetoelectronic devices such as magnetic tunnel junctions (MTJs). For TMR and GMR multilayers the interface properties (electronic states, spin polarization, roughness) at the ferromagnet–insulator interface are crucial parameters for the performance of the devices. In this case an uncontrolled formation of Co silicides ($CoSi_x$) at the cobalt–insulator interface has to be avoided.

2.3. Co-Growth with Ag Buffer Layer

To avoid $CoSi_x$ formation and to lower the film roughness, metallic buffer layers can be deposited on the H-passivated Si(111) substrate. For this propose Ag was chosen as the buffer layer because the growth of Ag on Si has already been studied[21,22] and the immiscibility of Ag with both Si[23] and Co[24] has been proved.

In Figure 5a a 200 Å Ag buffer layer grown on H-Si(111) at RT is shown. Atomically flat terraces with a local sixfold

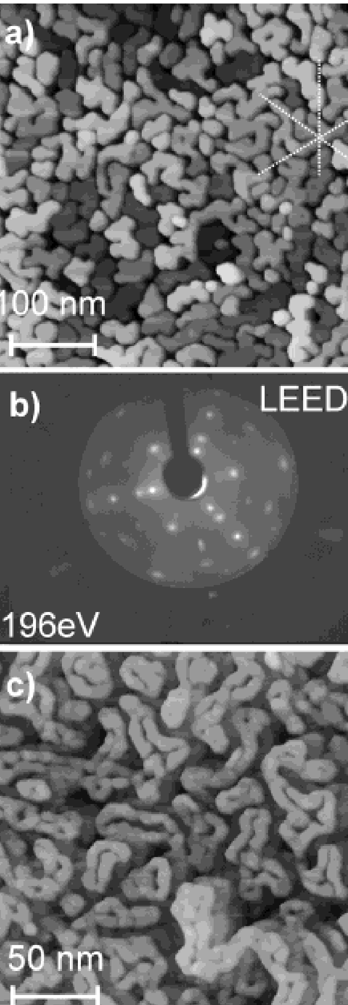

Fig. 5. a) STM image of a maze-like island structure with a sixfold in-plane symmetry (see dotted guidelines) of a nominally 200 Å thick Ag layer on a H-Si(111) substrate. b) The corresponding LEED pattern at an electron energy of 196 eV with a clear sixfold symmetry due to (111) orientation of the Ag layer. c) STM image of a nominally 200 Å thick Co layer on a (111)-oriented thick Ag buffer layer with a maze-like island structure. The Co cluster formation appears along the edges of the Ag islands.

in-plane symmetry (see dotted guidelines) can be seen due to a (111) orientation of the Ag layer. The low energy electron diffraction (LEED) pattern in Figure 5b of the Ag buffer layer shows also a sixfold symmetry, which confirms the (111) orientation of the Ag film on the H-passivated Si(111) surface. The lattice mismatch of a Ag(111) layer with a lattice parameter of 3.53 Å on the Si(111) surface with 3.89 Å is much smaller than in the case of Co(111) on Si(111). Nevertheless, the observed flat terraces are separated by deep trenches. The depth of the trenches could not be determined by STM, but in the corresponding Auger spectrum (not shown here) of the Ag film a clear Si Auger LMM transition was observed at an electron energy of 92 eV. As there is no intermixing between Si and Ag at RT, these trenches seem to go through the whole Ag layer.

Figure 5c shows the STM image of a 200 Å thick Co film on a 200 Å thick Ag buffer layer on a H-Si(111) substrate grown at RT. The growth of Co on top of the 200 Å thick Ag buffer layer leads to elongated Co clusters, which extend along the edges of the Ag islands. Here also, the deposition of a Ag buffer layer does not give the smoother and more homogeneous Co films necessary for ferromagnetic electrodes in magnetoelectronic devices.

2.4. Influence of Ag Deposition at Elevated Temperatures on the H-Passivated Si(111) Surface

The wet-chemically prepared H-Si(111)-(1×1) substrate was heated in UHV up to 550 °C and annealed for 40 min. Annealing at this temperature should lead to a complete desorption of the hydrogen from the H-Si(111) surface. Then 1 ML of Ag was deposited at 550 °C (hereafter this procedure will be called *hot deposition* of Ag). Once the Ag deposition had been finished, the temperature of the sample was maintained at 550 °C for 30 min. Then the sample was cooled down to RT. Figure 6 shows a STM image of the Si(111) surface resulting after hydrogen desorption followed by the hot deposition of Ag. Different dimer–adatom–stacking fault (DAS) structures with the periodicity of $(2n+1)\times(2n+1)$[25] can be found on the Si(111) surface, i.e., Si(111) 3×3, 5×5, 7×7, and 9×9 reconstructions. Magnifications of these reconstructions are shown in Figures 7a–d. A fragment of the Ag-Si(111)-(3×1) reconstruction[26] is also present on the surface (see Fig. 6). Such fragments were found over the whole surface investigated. No areas with a Ag-Si(111)-(√3×√3) reconstruction were observed on the sample surface. This may be due to the low coverage, i.e., 1 ML of Ag. For another sample with 3 ML of Ag deposited under the same conditions, large areas of a Ag-Si(111)-(√3×√3) reconstruction were found.

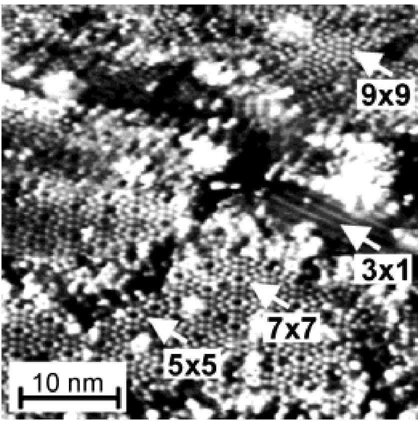

Fig. 6. STM image of a Si(111) surface after hydrogen desorption from a wet-chemically prepared H-Si(111)-(1×1) sample at 550 °C followed by the deposition of 1 ML Ag at the same temperature. The observable Ag/Si(111)-(3×1) and Si(111)-($(2n+1)\times(2n+1)$) reconstructions are marked by arrows.

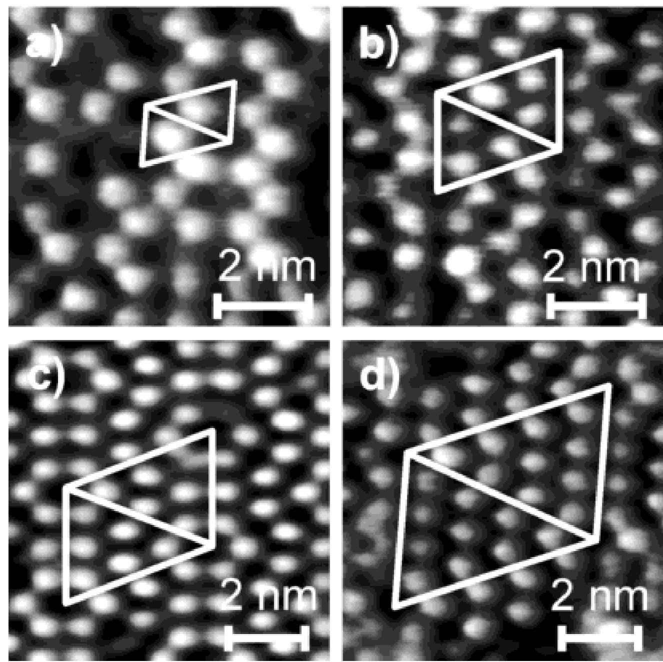

Fig. 7. Magnifications of observed reconstructions in Figure 6 after deposition of 1 ML Ag at 550 °C on the Si(111) surface (hot deposition of Ag): a) Si(111)-(3×3), b) Si(111)-(5×5), c) Si(111)-(7×7), and d) Si(111)-(9×9).

It is known that the Ag-Si(111)-(√3×√3) phase can be formed by Ag deposition on the 7×7 surface at temperatures in the range of 220–550 °C.[27,28] Around 550 °C Ag starts to desorb from the Ag-Si(111)-(√3×√3) surface. As Ag desorbs from the surface, 3×1 and 6×1 phases also generally appear, besides the √3×√3 structure, depending on the amount of Ag removed from the surface.[26] This means that the observed 3×1 reconstruction (Fig. 6) gives clear evidence of the existence of Ag on the sample surface. During the formation of 3×1 reconstruction areas the Si atoms are displaced by Ag and this may also be the source of the Si atoms.

The formation of the Ag-Si(111)-(√3×√3) phase is known to involve a substantial redistribution within the top Si(111) substrate layer (i.e., surface Si mass transport).[29] Silicon transport as evidenced by Ag–Si interaction[30–32] can be attributed to the enhancement of the surface migration of Si atoms under Ag irradiation at elevated temperatures. During the Ag evaporation onto the Si(111) substrate at 550 °C, Si atoms of the top substrate layers may be more mobile than without the Ag atom flux.

The disordered high-temperature "1×1" structure on the Si(111) surface is considered to be energetically closer to the

$\sqrt{3}\times\sqrt{3}$ reconstruction, because this disordered structure contains Si adatoms on the surface, as suggested by Yang and Williams.[33] According to theoretical total energy calculations, the difference of total energy between ideal 1×1 and 7×7 structures[34] and between ideal 1×1 and $\sqrt{3}\times\sqrt{3}$ structures[35] are 0.4 eV and 0.3 eV per 1×1 unit cell, respectively. The Ag on the Si(111)-(1×1) surface may induce Si adatom formation, which supports the formation of the DAS structures.

After the sample with a nominal coverage of 1 ML Ag on the surface was annealed at a temperature of 600 °C, Ag was desorbed from the surface. All the superstructures observed on this sample previously were converted into the almost perfect 7×7 reconstruction. The images obtained in pseudo-constant-height STM mode (high scan speed, feedback loop set to minimum) with a sample bias of –2.51 V showed a difference in the surface electronic states between the stacking faulted (SF) regions and stacking unfaulted (UF) regions in the 7×7 unit cell (not shown here). This proves that the images show the real 7×7 reconstruction.

The annealing temperature of 600 °C is far below the temperature at which the (1×1) → (7×7) transformation occurs (860 °C) and is also below the temperature of the 7×7 structure formation observed for thermal hydrogen desorption and annealing experiments at 700 °C on the wet processed H-Si(111) surface.[36] The possibility of 7×7 structure formation at temperatures lower than 700 °C was also shown by RHEED in the thermal H-desorption experiments on the wet-processed H-Si(111) surface.[37]

After deposition of nominally 3 ML Ag onto a wet-processed H-Si(111) surface at a temperature of only T = 250 °C (cold deposition of Ag), which is below the hydrogen desorption temperature (around 450 °C), Ag was thermally desorbed from the Ag/H-Si(111) surface. Here the Ag desorption temperature was chosen to be around 700 °C to ensure that the Ag is desorbed from the Ag-Si(111)-($\sqrt{3}\times\sqrt{3}$) surface. At a lower temperature of approximately 450 °C the hydrogen atoms first desorb from the Ag/H-Si(111) surface. Then, at around 550 °C, Ag forms the Ag-Si(111)-($\sqrt{3}\times\sqrt{3}$) reconstruction as shown in Figure 8.[38] After the desorption of the Ag from the Ag-Si(111)-($\sqrt{3}\times\sqrt{3}$) surface at a temperature between 600 °C and 700 °C a transition of the surface to the 7×7 reconstruction takes place. As a result of this annealing experiment a clear 7×7 reconstruction could be seen (inset in Fig. 8). The DAS structure was confirmed by resolving SF and UF regions of the 7×7 unit cell in the pseudo-constant-current mode with the same sample bias, –2.51 V. No evidence of other DAS structures such as 3×3, 5×5, and 9×9 was found. These measurements imply that the hot deposition of Ag energetically supports the formation of metastable Si(111)-(2n+1)×(2n+1) reconstructions.

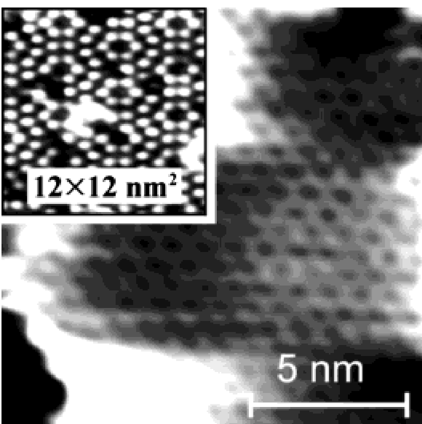

Fig. 8. STM image of the Si(111) surface (Ag/Si(111)-($\sqrt{3}\times\sqrt{3}$)) after the deposition of 3 ML Ag at T = 250 °C (cold deposition of Ag) and an annealing step at 550 °C for 40 min. The inset shows the same surface after additional annealing at T = 700 °C for 120 min; a clear Si(111) 7×7 reconstruction can be seen.

In order to elucidate the role of Ag in the formation of Si(111)-(2n+1)×(2n+1) reconstructions, annealing experiments on the wet-processed H-Si(111) were performed without Ag deposition.

Figure 9a shows a STM image of the H-Si(111)-(1×1) surface after annealing at 150 °C for 10 min. The 1×1 atomic arrangement of the hydrogen atoms is clearly seen and no significant change of the surface morphology after annealing was observed. The step height of the terraces of 3.1 Å ± 0.1 Å is the same as before annealing.

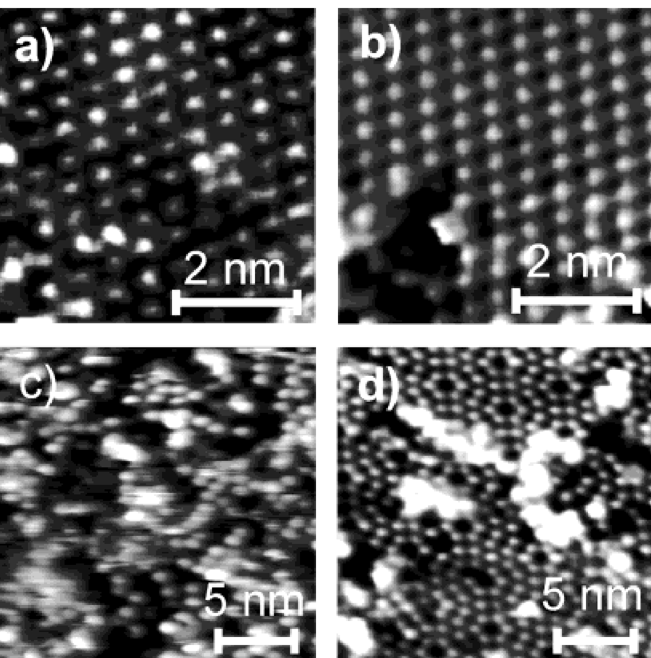

Fig. 9. STM image of a H-Si(111)-(1×1) surface a) after annealing at 150 °C for 10 min, b) after annealing at 300 °C for 15 min, c) distorted after annealing at 450 °C for 120 min, and d) converted into the Si(111) 7×7 reconstruction after annealing at 650 °C for 60 min.

After 15 min of additional annealing at 300 °C of the same sample the terrace shape and also the step height did not change, but a larger number of holes of different shape compared with the initial triangular etch-pits and irregularly shaped clusters appeared on the surface (Fig. 9b). The depth of the pits and the height of the clusters were the same as those on the H-Si(111) surface (around 3 Å) before annealing. The clusters were resolved atomically and again exhibited a 1×1 structure (not shown here). It can be seen in Figure 9b that the 1×1 structure is still well arranged without any perturbation

even if irregularly shaped pits and clusters exist. New pits might be formed by desorption of dihydride and trihydride from the surface followed by H-desorption around these defects.

Figure 9c shows the topography of the H-Si(111) surface after annealing at 450 °C for 2 h. The shapes of the steps and the terraces were preserved (not shown here) but the atomic arrangement changed remarkably and it seems that there is no long-range order as on the H-Si(111)-(1×1) surface. The clusters with a 1×1 structure disappeared, from which one can conclude that the clusters were neither contaminations (hydrocarbonates, carbides or metals) nor clusters of silicon oxide, which can normally be desorbed from the surface at temperatures significantly higher than 450 °C. Thus they consist of silicon atoms, which is consistent with the results of Komeda et al.[36] The structure becomes irregular and the surface looks very rough, but the root mean square (rms) roughness was almost the same as for the previously annealed surface shown in Figures 9a and b. Several fragments of the DAS structures can be found on the surface after annealing at 550 °C but the density of these structures is far lower than in the case of 1 ML hot-deposited Ag at 550 °C (see Figs. 6 and 7). This experiment shows that the hot deposition of Ag plays an important role in the energy of formation of Si(111)-($(2n+1)\times(2n+1)$) reconstructions.

After 1 h of additional annealing at 650 °C the surface was converted into an almost perfect 7×7 reconstruction (see Fig. 9d). The transformation temperature (annealing temperature) is higher than in the case of hot deposition of Ag. One can observe relatively tall clusters (maximum height 3.0 nm), which are thought to consist of silicon atoms, on top of a well-defined 7×7 reconstructed surface. These clusters are spread uniformly over the Si(111)-(7×7) surface. Although there exist some defects in the 7×7 structure, the images show the same structure as obtained by known methods.[39–41] The presence of silicon clusters might explain why no clear 7×7 diffraction patterns of this sample have yet been resolved using LEED and RHEED techniques.

3. Conclusion

To summarize, Co growth on H-passivated Si(111) was found to occur by the Vollmer–Weber (3D) growth mode at RT, leading to a surface with a peak-to-peak roughness of 18 Å for a 200 Å thick Co film. In the case of an increased growth temperature of $T = 100$ °C, cobalt silicide is formed. The deposition of a Ag buffer layer does not reduce the peak-to-peak roughness or increase the homogeneity of a following Co layer. The performance of TMR and GMR components and devices grown on H-passivated Si(111) substrates in UHV should be investigated in the future.

Various DAS superstructures, such as 3×3, 5×5, 7×7, and 9×9, were observed on the Si(111) surface after the deposition of 1 ML Ag at a substrate temperature of 550 °C. All the metastable structures convert into the 7×7 reconstruction after additional annealing at 600 °C. After Ag deposition at a substrate temperature of $T = 250$ °C followed by annealing at 550 °C no metastable DAS structures were found on the surface. Hydrogen thermal desorption experiments also did not show extensive formation of DAS structures at temperatures near 550 °C.

4. Experimental

Thin film deposition by molecular beam epitaxy (MBE) and in situ characterization of the samples were carried out using two different UHV systems. The first was an Omicron Surface Science UHV system with a base pressure of 8×10^{-11} mbar equipped with an in situ atomic force microscope and a scanning tunneling microscope as well as electron beam evaporators. The second system was an UHV MBE system with a base pressure of 8×10^{-11} mbar. It was equipped with electron beam evaporators and Knudsen cells for thin film deposition, and in addition in situ STM [42,43], AES, LEED, RHEED, and X-ray photoelectron spectroscopy (XPS) experiments were possible.

The substrates were rectangular (10 mm × 4 mm × 0.375 mm) cut from a B-doped p-type Si(111) wafer (4.5 Ω cm) within an out-of-plane misorientation angle of ±0.5° miscut. The sample cleaning and hydrogen (H) termination were carried out in accordance with the wet-chemical etching procedure described by Higashi et al. [44]. This preparation procedure is known to yield an ideal monohydride-terminated Si(111) surface [12]. After the preparation process the samples were transferred to a load–lock chamber and pumped down by an oil-free prepump and a turbomolecular pump within 30 min. The samples were introduced into the UHV chamber after the pressure in the load-lock reached 1×10^{-7} mbar.

The H-Si(111) samples were heated using a radiative heater placed behind the sample holder while the pressure was kept below 5×10^{-9} mbar. The temperature was monitored by a chromel–alumel thermocouple located between the heater and the sample holder. The absolute accuracy of the temperature measurements was ±20 °C. After each heating process the samples were slowly cooled down to room temperature (cooling speed less than 0.5 °C/s).

All STM measurements were carried out at room temperature using electrochemically etched polycrystalline tungsten tips cleaned in UHV by Ar^+ ion sputtering.

Received: November 24, 2000
Final version: February 5, 2001

[1] M. N. Baibich, J. M. Broto, A. Fert, F. Nguyen van Dau, F. Petroff, P. Etienne, G. Creuzet, A. Friederich, J. Chazelas, *Phys. Rev. Lett.* **1988**, *61*, 2427.
[2] G. Binasch, P. Grünberg, F. Saurenbach, W. Zinn, *Phys. Rev. B* **1989**, *39*, 4828.
[3] S. S. P. Parkin, N. More, K. P. Roche, *Phys. Rev. Lett.* **1990**, *64*, 2304.
[4] J. S. Moodera, L. R. Kinder, T. M. Wong, R. Meservey, *Phys. Rev. Lett.* **1995**, *74*, 3273.
[5] S. S. P. Parkin, K. P. Roche, M. G. Samant, P. M. Rice, R. B. Beyers, R. E. Scheuerlein, E. J. O'Sullivan, S. L. Brown, J. Bucchigano, D. W. Abraham, Y. Lu, M. Rooks, P. L. Trouilloud, R. A. Wanner, W. J. Gallagher, *J. Appl. Phys.* **1999**, *85*, 5828.
[6] M. Julliére, *Phys. Lett. A* **1975**, *54*, 225.
[7] P. Zahn, J. Binder, I. Mertig, R. Zeller, P. H. Dederichs, *Phys. Rev. Lett.* **1998**, *80*, 4309.
[8] C. Blaas, P. Weinberger, L. Szunyogh, P. M. Levy, C. B. Sommers, *Phys. Rev. B* **1999**, *60*, 492.
[9] J. Kudrnovsky, V. Drchal, C. Blaas, I. Turek, P. Weinberger, *Phys. Rev. Lett.* **1996**, *76*, 3834.
[10] I. I. Oleinik, E. Y. Tsymbal, D. G. Pettifor, *Phys. Rev. B* **2000**, *62*, 3952.
[11] P. Mavropoulos, N. Papanikolaou, P. H. Dederichs, *Phys. Rev. Lett.* **2000**, *85*, 1088.
[12] P. Dumas, Y. J. Chabal, G. S. Higashi, *Phys. Rev. Lett.* **1990**, *65*, 1124.
[13] J. Camarero, L. Spendeler, G. Schmidt, K. Heinz, J. J. de Miguel, R. Miranda, *Phys. Rev. Lett.* **1994**, *73*, 2448.
[14] W. F. Egelhoff, M. T. Kief, *Phys. Rev. B* **1992**, *45*, 7795.
[15] W. J. Gallagher, S. S. P. Parkin, Y. Lu, X. P. Bian, A. Marley, K. P. Roche, R. A. Altmann, S. A. Rishton, C. Jahnes, T. M. Shaw, G. Xiao, *J. Appl. Phys.* **1997**, *81*, 3741.
[16] T. Zhu, R. Swanson, presented at *43rd Conf. on Magnetism and Magnetic Materials*, Miami, FL **1998**.
[17] K. Kaji, S.-L. Yau, K. Itaya, *J. Appl. Phys.* **1995**, *78*, 5727.
[18] F. Nouvertné, U. May, M. Bamming, A. Rampe, U. Korte, G. Güntherodt, R. Pentcheva, M. Scheffler, *Phys. Rev. B* **1999**, *60*, 14 382.

[19] M. Scheffler, C. Stampfl, in *Handbook of Surface Science*, Vol. 2 (Eds: K. Horn, M. Scheffler), Elsevier, Amsterdam **1999**.
[20] J. Derrien, M. De Crescenzi, E. Chainet, C. d'Anterroches, *Phys. Rev. B* **1987**, *36*, 6681.
[21] M. Naitoh, A. Watanabe, S. Nishigaki, *Surf. Sci.* **1996**, *357–358*, 140.
[22] G. van Tendeloo, X. B. Zhang, A. L. Vasiliev, Y. He, L.-M. Yu, P. A. Thiry, *Surf. Sci.* **1995**, *340*, 317.
[23] *Binary Alloy Phase Diagrams*, Vol. 1 (Ed: T. B. Massalski), ASM International, Materials Park, OH **1996**, p. 93.
[24] *Binary Alloy Phase Diagrams*, Vol. 1 (Ed: T. B. Massalski), ASM International, Materials Park, OH **1996**, p. 25.
[25] K. Takayanagi, Y. Tanishiro, M. Takahasi, S. Takahashi, *J. Vac. Sci. Technol. A* **1985**, *3*, 1502.
[26] K. J. Wan, X. F. Lin, J. Nogami, *Phys. Rev. B* **1992**, *46*, 13 635.
[27] H. Ohnishi, I. Katayama, Y. Ohba, F. Shoji, K. Oura, *Jpn. J. Appl. Phys.* **1993**, *32*, 2920.
[28] G. LeLay, *Surf. Sci.* **1983**, *132*, 169.
[29] A. A. Saranin, A. V. Zotov, V. G. Lifshits, J. T. Ryu, O. Kubo, H. Tani, T. Harada, M. Katayama, K. Oura, *Surf. Sci.* **1999**, *429*, 127.
[30] A. Shibata, Y. Kimura, K. Takayanagi, *J. Vac. Sci. Technol. B* **1994**, *12*, 2026.
[31] W. McComb, D. J. Moffatt, P. A. Hackett, B. R. Williams, B. F. Mason, *Phys. Rev. B* **1994**, *49*, 17139.
[32] A. Shibata, Y. Kimura, K. Takayanagi, *Surf. Sci.* **1994**, *303*, 161.
[33] Y. N. Yang, E. D. Williams, *Phys. Rev. Lett.* **1994**, *72*, 1862.
[34] G.-X. Qian, D. J. Chadi, *Phys. Rev. B* **1987**, *35*, 1288.
[35] G.-X. Qian, D. J. Chadi, *J. Vac. Sci. Technol. B* **1986**, *4*, 1079.
[36] T. Komeda, Y. Morita, H. Tokumoto, *Surf. Sci.* **1996**, *348*, 153.
[37] Le Tanh Vinh, M. Eddrief, C. A. Sebenne, P. Dumas, A. Taleb-Ibrahimi, R. Gunther, Y. J. Chabal, J. Derrien, *Appl. Phys. Lett.* **1994**, *64*, 3308.
[38] In this case we deposited nominally 3 ML of Ag, so only some of the deposited Ag took part in the formation of the Ag–Si(111)-($\sqrt{3}\times\sqrt{3}$) phase and the remaining Ag would be clustered on the Ag–Si(111)-($\sqrt{3}\times\sqrt{3}$) surface.
[39] K. Takahashi, C. Nara, T. Yamagishi, T. Onzawa, *Appl. Surf. Sci.* **1999**, *151*, 299.
[40] P. A. Bennet, M. B. Webb, *Surf. Sci.* **1981**, *104*, 74.
[41] S. Kitamura, T. Sato, M. Iwatsuki, *Nature* **1991**, *351*, 215.
[42] K. Besocke, *Surf. Sci.* **1987**, *181*, 145.
[43] J. Frohn, J. F. Wolf, K. Besocke, M. Teske, *Rev. Sci. Instrum.* **1989**, *60*, 1200.
[44] G. S. Higashi, Y. J. Chabal, G. W. Trucks, K. Raghavarachi, *Appl. Phys. Lett.* **1990**, *56*, 656.